Seismic reflection imaging of large-amplitude lee waves in the Caribbean Sea

Dan Eakin,[1,2] W. S. Holbrook,[1] and Ilker Fer[3]

Received 4 August 2011; revised 22 September 2011; accepted 23 September 2011; published 1 November 2011.

[1] Results from the first testing of the *R/V Marcus Langseth* as a platform for collecting seismic reflection data from the water column of the ocean demonstrate that large-amplitude lee waves can be acoustically mapped. A seismic profile collected in the Caribbean Sea offshore Costa Rica shows disturbances in finestructure, which we interpret to be lee waves, propagating hundreds of meters vertically through the water column above seafloor ridges. Waves show vertical displacements of 30–50 m and horizontal wavelengths of 300–3000 m. Reflector displacement spectra calculated in the region containing the lee waves exceed Garrett-Munk energy levels by up to a factor of 10 at horizontal wavelengths of 300–3000 m, suggesting a locally derived source of internal wave energy consistent with our interpretation. Our results show that it is possible to image large-scale lee waves, a phenomenon potentially responsible for dissipation and mixing within the ocean. **Citation:** Eakin, D., W. S. Holbrook, and I. Fer (2011), Seismic reflection imaging of large-amplitude lee waves in the Caribbean Sea, *Geophys. Res. Lett.*, *38*, L21601, doi:10.1029/2011GL049157.

1. Introduction

[2] Small scale mixing processes in the ocean play an important, but poorly understood, role in ocean circulation and mixing. Ocean mixing phenomena are typically sampled using acoustics, expendable instruments, tethered instruments, towed instruments, autonomous instruments, and satellite images. Recently, a new means of visualizing ocean finestructure, seismic oceanography [*Holbrook et al.*, 2003], has been developed. Within the past few years seismic oceanography has been used to image various oceanographic phenomena, including turbulence [*Sheen et al.*, 2009], fronts and thermohaline intrusions [*Holbrook et al.*, 2003; *Tsuji et al.*, 2005; *Nakamura et al.*, 2006], thermohaline staircases [*Fer et al.*, 2010], meso-scale eddies [*Biescas et al.*, 2008; *Ruddick et al.*, 2009], and strain caused by internal gravity waves [*Nandi et al.*, 2004; *Holbrook and Fer*, 2005; *Krahmann et al.*, 2008; *Holbrook et al.*, 2009]. These studies have proven the ability of seismic oceanography to image large-scale oceanographic processes and properties. Used in conjunction with conventional high-resolution sampling methods (tows, expendable instruments etc.), seismic oceanography has the potential to provide complete regional-scale physical characterization of oceanic processes while simultaneously measuring the process locally using conventional sampling methods.

[3] Recently high-mode lee waves have been observed at underwater ridges and continental shelves [*Klymak et al.*, 2010]. Similar phenomena associated with mixing have been imaged over a shallow sill with high-frequency acoustics in the Knight Inlet [*Farmer and Smith*, 1980] and Oregon continental slope [*Nash et al.*, 2007]. Observations and numerical simulations by *Edwards et al.* [2004] show lee waves to be a source of form drag turbulence over sharp topography, and may be one of the primary mechanisms for extracting energy from barotropic currents. Furthermore, the ability of radiating internal waves (including lee waves) to dissipate significant amounts of barotropic tidal energy and concentrate regions of intense vertical mixing suggest they may have a more important role in the ocean energy budget then previously thought [*Nash et al.*, 2007].

[4] In this study, we present evidence that seismic reflection profiling has imaged for the first time large-amplitude internal lee waves along sharp topography. Our study provides a detailed 2D seismic image over a 155-km-long profile in the Caribbean Sea, parallel to the east coast of Costa Rica. We focus on a 12-km-long section that shows near-vertical disturbances propagating from sharp topography disrupting continuous water column reflections, which we interpret to be standing lee waves produced by steady state current flow over sharp topography.

2. Setting

[5] The Caribbean Sea consists of a dynamic circulation system driven in the east by the Caribbean current bringing water from the equatorial Atlantic via the North Equatorial, North Brazil, and Guiana currents. The Panama-Colombia Gyre, evident offshore Central America, flows counterclockwise within the Colombia Basin (Figure 1). Current velocities produced by the gyre vary with water depth and are strongest in the upper 50 m, but are still perceptible at depths approaching 800 m [*Andrade et al.*, 2003]. Gyre currents directly measured by satellite-tracked drift buoys in our study area during 1998–2000 recorded north to south surface current velocities parallel to the eastern coast of Costa Rica between 60 and 100 cm s^{-1} [*Richardson*, 2005]. The magnitude and direction of the currents coupled with the sharp submarine topography in our study area are ideal for the generation of lee waves in the orientations we observe in the seismic section.

3. Methods

[6] Seismic data used in this study were acquired in February 2008 using the *R/V Marcus Langseth* in the

[1]Department of Geology and Geophysics, University of Wyoming, Laramie, Wyoming, USA.
[2]Now at Institute for Geophysics, University of Texas at Austin, Austin, Texas, USA.
[3]Geophysical Institute, University of Bergen, Bergen, Norway.

Copyright 2011 by the American Geophysical Union.
0094-8276/11/2011GL049157

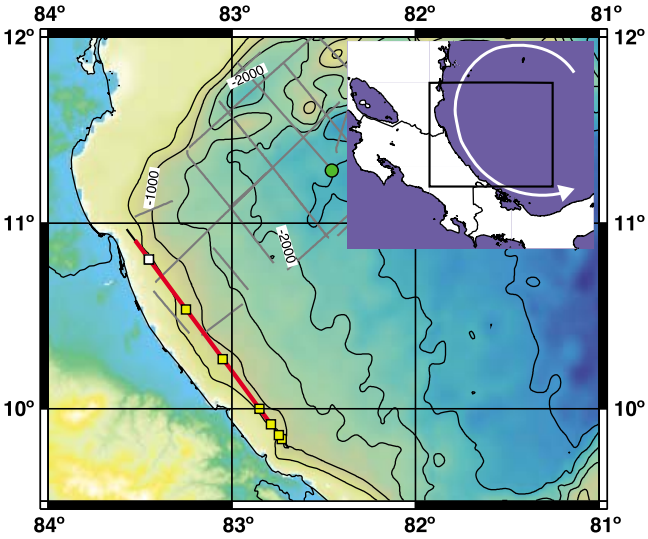

Figure 1. Bathymetric map of the study area in the Caribbean Sea including locations of all seismic reflection transects acquired (gray lines). Red line shows extent of the seismic reflection transect (Limon2) used in this study (Figure 2). Yellow squares show locations of XBT deployed along the transect; white square shows location of the XBT instrument used in this study; green circle shows location of XCTD from which buoyancy frequency was calculated. Inset shows location of the survey; white arrow shows general path of the Panama-Colombia Gyre, after *Richardson* [2005].

Caribbean Sea as part of the TICO-CAVA project. Acoustic energy was produced from 36 air guns with a combined volume of 6600 cubic inches fired every 50 m. An eight-km-long streamer containing 636 hydrophone groups was towed behind the ship resulting in a horizontal subsurface sampling spacing of 6.25 m. Reflected energy was sampled every 2 ms.

[7] Conventional seismic processing steps were applied, including trace editing, velocity analysis, stacking, bandpass filtering and post-stack time migration to create the final seismic profile (Figure 2). Water column reflections were migrated separately from subsurface geology to reduce migration artifacts [*Nandi et al.*, 2004].

[8] Five Sippican T-5 XBT and four T-7 XBT probes were deployed at an average horizontal spacing of 4 km during the first half of seismic acquisition and an average of 36 km during the latter half of acquisition. Ocean temperature was sampled by the XBT's approximately every 0.7 m in the vertical. The resulting temperature profiles were used, together with T-S relationships from a nearby XCTD, to calculate buoyancy frequency (N), used later to calculate the vertical mode of the lee waves observed in the section.

4. Results and Discussion

[9] A migrated seismic reflection profile of the Limon2 transect clearly shows tilted, near-vertical disturbances in water column reflections above the southern slope of topographic ridges at depths up to 700 m that we interpret to be lee waves (Figures 2 and 3). A north to south flow direction (from left to right in the seismic profile) would be ideal to generate upstream tilted lee waves on the southern (down current) side of topography, as observed in the seismic image. Studies referenced by *Richardson* [2005] show currents in this area having strong north to south trajectories and high surface velocities (60–100 cm/sec) whose effect may extend to several hundred meters, suggesting the vertical disturbances in the seismic image are lee waves generated as a result of steady-state current forcing over rough topography.

[10] Modeling of lee wave generation produced by *Klymak et al.* [2010] shows generation of lee waves over sharp topography, due to steady state current forcing (Figure 3), a situation similar to the processes controlling lee wave generation in our study area. The lee wave response is a function of the mode of flow over the topography given by Nh_m/U_o, where N is the buoyancy frequency, h_m the height of the topography from the channel floor, and U_o the flow speed infinitely far from the obstacle [*Klymak et al.*, 2010]. For moderate $8 > Nh_m/U_o, \geq 1$ (low mode), a tilted vertical response propagates far up and downstream of the obstacle, and an arrested lee wave forms at the topography and tilts upstream [*Klymak et al.*, 2010].

[11] Using the equation above, a representative range of flow velocities between U_o = 0.1 m s^{-1} and 0.2 m s^{-1} (P. Richardson, personal communication, 2008) and an average buoyancy frequency of N = 5.17 × 10^{-3} s^{-1} calculated from an XCTD profile collected during seismic acquisition (Figure 1), we calculated the mode of the lee wave over the topography of interest (h_m between 80 and 100 m) to be between 4.2 and 4.4 (low mode). The stratification here is approximately equal to the $N \sim 5.2 \times 10^{-3}$ s^{-1} used in *Klymak et al.*'s [2010] model to simulate low mode lee wave generation.

[12] We interpret the observed sharp undulations in otherwise continuous water column reflections to be the result of large-amplitude lee waves propagating vertically through the water column disrupting isopycnals (Figure 3). The average resolvable magnitude of vertical displacement of the waves is between 30 and 50 m. The horizontal wavelengths of the disturbances (~300–1000 m) are comparable to the width of the topography beneath the disturbances. *Klymak et al.* [2010] show that in a finite-depth fluid, low-mode large amplitude

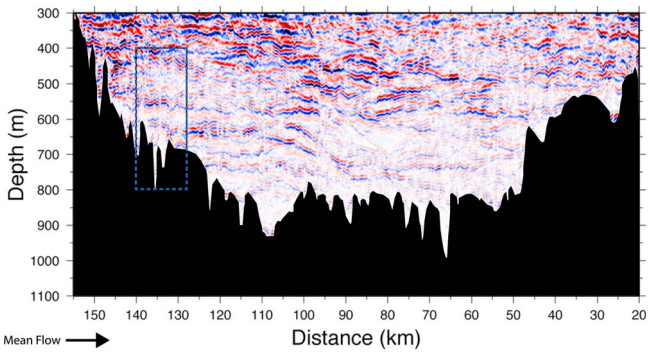

Figure 2. 135 km stacked section of the Limon2 transect. Mean flow direction is from left to right (approximately north to south) in the section. Blue-black dotted box outlines 400–800 m × 12 km area where interpreted large amplitude lee waves appear to propagate vertically through the water column from the lee side of sharp topography.

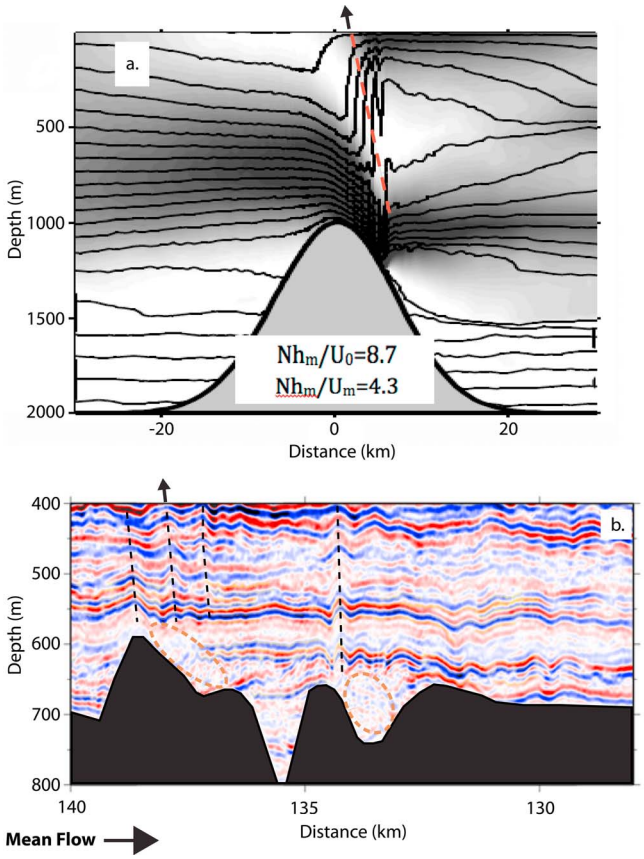

Figure 3. (a) Numerical modeling from *Klymak et al.* [2010] showing the generation of a low mode large amplitude lee wave resulting from steady state of moderate Nh_m/U_0 flow. Contours are of density and shading represents fast and slow-moving water. Dotted line traces the peak phase velocity of the modeled lee wave slightly tilted in the upstream direction. Arrow at the top of the figure represents the group velocity directed upwards resulting from the downward tilting orientation of the phase velocity. Flow in both panels is from left to right. (b) Zoom of our study area outlined in Figure 2 showing several disturbances in water column reflections propagating several hundred meters above topographic ridges. Black-dotted lines trace the phase velocities of several waves slightly tilted in the upstream direction with the black arrow representing the group velocity directed upwards as in Figure 3a. Two acoustically transparent packages (orange dotted circles) are observed on the lee side of sharp topography generating lee waves that we interpret to be turbulence caused by breaking internal waves off the slopes of the topography.

nonlinear lee waves are of similar scale to the topography generating them if the phase speed is equal and opposite to the generating current [*Baines*, 1997]. Our results support the previous statement based on the wavelengths of the observed lee waves in the seismic section, which are comparable to the width of the topography generating them, coupled with a low vertical mode of the waves calculated in our study area. One more piece of evidence for our interpretation is the slightly backwards-leaning peak phase of each undulation as it propagates vertically through the water column (dotted lines in Figure 3). This is a well-known feature of internal lee waves derived from the phase/group velocities of such waves (see *Gill* [1982] for derivation). Lee waves appear stationary with respect to the bathymetric feature over which they are radiating, resulting in a pattern of wave crests and troughs that "tilt" backwards in the upstream direction. The resulting group velocity (arrows in Figure 3) is denoted by a vertical energy flux that represents the energy lost from the flow due to internal wave drag. Interpreted lee wave trajectories can be inferred from reflector undulations originating from topography at depths of 600 – 700 m and can be tracked vertically, tilting in the upstream direction for several hundred meters in our seismic section. Substantial vertical displacement over such a specific range of wavelengths is indicative of enhanced internal wave energy at these wavelengths. If a local source of internal wave energy is present, we expect to see anomalous reflector displacement spectra in the section containing the vertical disturbances.

[13] Horizontal wavenumber reflector displacement spectra were calculated as by *Holbrook and Fer* [2005]. We show mean displacement spectra (Figure 4) from reflectors at 50–130 km horizontal offset (500–700 m depth), and 30–130 km horizontal offset (300–500 m depth) corresponding to the region of the seismic profile we do not observe lee wave energy (Figure 2). We also show spectra at 130–150 km horizontal offset (300–500 m and 500–700 m depth) from the region of the seismic profile associated with observed lee waves (Figures 2 and 3). All calculated spectra are compared with the Garrett-Munk tow spectrum, version GM76 as described by *Katz and Briscoe* [1979]. In order to account for varying stability with depth, spectra are scaled with the buoyancy frequency N(z) [see *Katz and Briscoe*, 1979, equation A10]. We use N = 1.6 cycles per hour (cph), which is the mean N for the 500–700 depth range on the nearby XCTD (Figure 1). Because isopycnal displacements are vertically correlated, the displacement spectra inferred from vertically adjacent reflectors are not independent. The degrees of freedom (DoF) are determined by assuming that every eighth spectrum is truly independent, yielding DoF between 45 and 55 for the segments away from the area with the lee wave signature. For the segments suggestive of lee wave structure, DoF = 41 for 300–500 m range and DoF = 24 for 500–700 m range. The key observation is that the profiles where we do not observe internal lee waves generate spectra in good agreement with GM76, whereas spectra generated from reflections in the section containing interpreted lee waves (Figures 3 and 4) show substantially enhanced spectral levels at horizontal wavelengths of 250–3000 m, reaching nearly an order of magnitude greater than GM76 at 500–1000 m wavelength (Figure 4). Such strongly enhanced spectral levels at horizontal wavelengths comparable to those of the underlying topography strongly suggest a locally derived source of internal wave energy. These results are consistent with our interpretation that the tilted vertical disturbances of the reflectors are the result of large-amplitude lee waves present within the section.

[14] Regions of seismically transparent water are present on the down-slope, downstream sides of the topography generating lee waves (Figure 3). We interpret these to be areas of high turbulence resulting from breaking internal waves from fluid flow over the crest of the topography. This interpretation is based on the observation that several strong

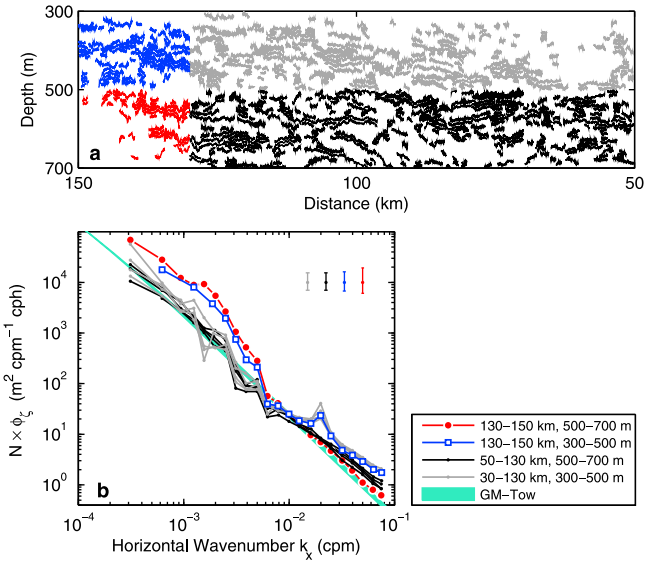

Figure 4. (a) Representative section showing all reflectors used to generate the horizontal wavenumber displacement spectra shown in Figure 4b. (b) All reflector displacement spectra plotted against the GM76-tow (green line) scaled by the buoyancy frequency N(z) [*Katz and Briscoe*, 1979, equation A10]. Reflectors away from the region containing interpreted lee waves (50–130 km (black reflectors in Figure 4a) and 30–130 km (gray reflectors in Figure 4a) generate spectra in agreement with GM76. Spectra generated from reflectors in the area containing lee waves (130–150 km (red reflectors in Figure 4a) and 130–150 km (blue reflectors in Figure 4a) show enhanced spectral levels at wavelengths of 250–3000 m, reaching close to an order of magnitude greater than GM76 at 500–1000 m wavelengths. Corresponding errorbars are determined by assuming every 8th spectra is truly independent. Resulting DoFs for spectra between 50–130 km and 30–130 km vary between 45 and 55, and we used DoF = 50, representative for these spectra. For the 130–150 km segments, DoF = 41 for 300–500 m range and DoF = 24 for 500–700 m range. DoF are valid for the low wavenumbers and tighter for larger wavenumbers due to wavenumber band averaging.

coherent reflectors are disrupted as they enter these areas, implying some level of turbulence is responsible. These observations suggest that seismic reflection profiling could provide an important complement to process-oriented studies of the causes and consequences of lee wave generation.

5. Conclusions

[15] The results of this study indicate that seismic reflection profiling can image large-amplitude lee waves propagating vertically through the water column at great depths. Displacements in water column reflections, which appear to correlate over hundreds of meters vertically, mimic (at least qualitatively) the predicted vertical, upstream-tilted geometries of lee waves modeled by *Klymak et al.* [2010]. There is a direct relationship between the wavelength of lee waves in the section and enhanced spectral energy at those wavelengths, implying that future studies may be able to use similar measurements of internal wave energy to remotely estimate and quantify mixing in these areas. The extraordinary ability of seismic reflection imaging to provide fine vertical and horizontal resolution of the water column of the ocean can lead to new insights into oceanic mixing phenomena at greater depths.

[16] **Acknowledgments.** We thank the crew of the *R/V Marcus Langseth* for a successful cruise, R. Schmitt, P. Richardson, and J. Klymak for helpful conversations, and H. van Avendonk, W. Fortin and J. Marson for data acquisition. Data were processed using Paradigm's Focus software and Generic Mapping Tools. Supported by the National Science Foundation's Physical Oceanography and MARGINS programs, under grants OCE-0405654 and OCE-0648620.

[17] The Editor thanks Barry Ruddick and an anonymous reviewer for their assistance in evaluating this paper.

References

Andrade, C. A., E. D. Barton, and C. N. K. Mooers (2003), Evidence for an eastward flow along the Central and South American Caribbean coast, *J. Geophys. Res.*, *108*(C6), 3185, doi:10.1029/2002JC001549.

Baines, P. G. (1997), Topographic effects in stratified flows, Cambridge University Press.

Biescas, B., V. Sallares, J. Pelegri, F. Machin, R. Carbonell, G. Buffett, J. Danobeitia, and A. Calahorrano (2008), Imaging meddy finestructure using multichannel seismic reflection data, *Geophys. Res. Lett.*, *35*, L11609, doi:10.1029/2008GL033971.

Edwards, K. A., P. MacCready, J. N. Moum, G. Pawlak, J. M. Klymak, and A. Perin (2004), Form Drag and Mixing Due to Tidal Flow past a Sharp Point, *Journal of Physical Oceanography*, *34*, 1297–1312.

Farmer, D. M., and J. D. Smith (1980), Tidal interaction of stratified flow with a sill in Knight Inlet, *Deep Sea Res., Part A*, *27*, 239–254, doi:10.1016/0198-0149(80)90015-1.

Fer, I., P. Nandi, W. S. Holbrook, R. W. Schmitt, and P. Páramo (2010), Seismic imaging of a thermohaline staircase in the western tropical North Atlantic, *Ocean Sci.*, *6*, 621–631, doi:10.5194/os-6-621-2010.

Gill, A. E. (1982), *Atmosphere-Ocean Dynamics*, Academic, New York.

Holbrook, W. S., and I. Fer (2005), Ocean internal wave spectra inferred from seismic reflection transects, *Geophys. Res. Lett.*, *32*, L15604, doi:10.1029/2005GL023733.

Holbrook, W. S., P. Paramo, P. Pearse, and R. W. Schmitt (2003), Thermohaline fine structure in an oceanographic front from seismic reflection profiling, *Science*, *301*, 821–824, doi:10.1126/science.1085116.

Holbrook, W. S., I. Fer, and R. W. Schmitt (2009), Images of internal tides near the Norwegian continental slope, *Geophys. Res. Lett.*, *36*, L00D10, doi:10.1029/2009GL038909.

Katz, E., and M. G. Briscoe (1979), Vertical coherence of the internal wave field from towed sensors, *J. Phys. Oceanogr.*, *9*, 518–530, doi:10.1175/1520-0485(1979)009<0518:VCOTIW>2.0.CO;2.

Klymak, J. M., S. M. Legg, and R. Pinkel (2010), High-mode stationary waves in stratified flow over large obstacles, *J. Fluid Mech.*, *644*, 321–336, doi:10.1017/S0022112009992503.

Krahmann, G., P. Brandt, D. Klaeschen, and T. Reston (2008), Mid-depth internal wave energy off the Iberian Peninsula estimated from seismic reflection data, *J. Geophys. Res.*, *113*, C12016, doi:10.1029/2007JC004678.

Nakamura, Y., T. Noguchi, T. Tsuji, S. Itoh, H. Niino, and T. Matsuoka (2006), Simultaneous seismic reflection and physical oceanographic observations of oceanic fine structure in the Kuroshio extension front, *Geophys. Res. Lett.*, *33*, L23605, doi:10.1029/2006GL027437.

Nandi, P., W. S. Holbrook, S. Pearse, P. Paramo, and R. W. Schmitt (2004), Seismic reflection imaging of water mass boundaries in the Norwegian Sea, *Geophys. Res. Lett.*, *31*, L23311, doi:10.1029/2004GL021325.

Nash, J. D., M. H. Alford, E. Kunze, K. Martini, and S. Kelley (2007), Hotspots of deep-ocean mixing on the Oregon continental slope, *Geophys. Res. Lett.*, *34*, L01605, doi:10.1029/2006GL028170.

Richardson, P. L. (2005), Caribbean Current and eddies as observed by surface drifters, *Deep Sea Res., Part II*, *52*, 429–463, doi:10.1016/j.dsr2.2004.11.001.

Ruddick, B., H. B. Song, C. Z. Dong, and L. Pinheiro (2009), Water column seismic images as maps of temperature gradient, *Oceanography*, *22*, 192–205, doi:10.5670/oceanog.2009.19.

Sheen, K. L., N. J. White, and R. W. Hobbs (2009), Estimating mixing rates from seismic images of oceanic structure, *Geophys. Res. Lett.*, *36*, L00D04, doi:10.1029/2009GL040106.

Tsuji, T., T. Noguchi, H. Niino, T. Matsuoka, Y. Nakamura, H. Tokuyama, S. Kuramoto, and N. Bangs (2005), Two-dimensional mapping of fine

structures in the Kuroshio Current using seismic reflection data, *Geophys. Res. Lett.*, *32*, L14609, doi:10.1029/2005GL023095.

D. Eakin, Institute for Geophysics, University of Texas at Austin, 10100 Burnet Rd., Austin, TX 78758-4445, USA. (deakin01@gmail.com)

I. Fer, Geophysical Institute, University of Bergen, Allegaten 70, N-5007 Bergen, Norway.

W. S. Holbrook, Department of Geology and Geophysics, University of Wyoming, 1000 E. University Ave., Laramie, WY 82071-3006, USA.